Doppler Spectroscopy of OH Fragments from the Photodissociation of HOCl at 266 and 355 nm

Hisashi Fujiwara and Takashi Ishiwata*

Department of Information Machines and Interfaces, Faculty of Information Sciences, Hiroshima City University, Hiroshima 731-3194, Japan

Received: January 6, 1998; In Final Form: March 26, 1998

Photofragment Doppler spectroscopy has been used to characterize the electronically excited states of HOCl in the ultraviolet region. In the photolysis of HOCl, the Doppler profile of the nascent OH fragments shows a marked difference in the recoil anisotropy parameters: $\beta = 1.31 \pm 0.12$ at 266 nm and -0.70 ± 0.12 at 355 nm. Photoabsorption at 266 nm is characterized by the transition moment predominantly parallel to the O−Cl axis, which is consistent with assignment of the strong band at 250 nm to the $2^1A'-1^1A'$ transition. On the other hand, the transition moment at 355 nm is perpendicular to the O−Cl bond. The measurement of the rotational alignment also shows the transition moment to be perpendicular to the molecular plane at 355 nm, indicating the existence of the $1^1A'' \leftarrow 1^1A'$ transition above 300 nm.

1. Introduction

Hydrochlorous acid (HOCl) has recently received much attention because of its possibility for a reservoir of atmospheric chlorine.[1] It is suggested to be formed in the stratosphere homogeneously,

$$HO_2 + ClO \rightarrow HOCl + O_2 \quad (1)$$

and heterogeneously in the polar stratospheric clouds during the winter.[2,3]

$$ClONO_2 + H_2O \rightarrow HOCl + HNO_3 \quad (2)$$

HOCl has an absorption spectrum in the ultraviolet region, and the photolysis is believed to dominate a removal of HOCl.[4]

The following photolysis processes are energetically possible:[5]

$$HOCl + h\nu \rightarrow O(^3P) + HCl(X^1\Sigma) \qquad \lambda < 510 \text{ nm} \quad (3)$$

$$\rightarrow Cl(^2P) + OH(X^2\Pi) \qquad \lambda < 500 \text{ nm} \quad (4)$$

Reaction 4 was identified to occur predominantly above 300 nm.[6−8] Most of the experimental spectra showed a strong band peaked at ∼250 nm with a shoulder above 300 nm, but the spectral profiles and absorption cross sections did not agree with each other.[9−12] This is especially true in the spectrum above 300 nm, which is important to estimate the lifetime of HOCl in the stratosphere since the solar flux above 300 nm is dominant. Ab initio calculations have been performed to predict the spectrum, and the dissociation dynamics in the electronically excited states has been discussed.[13−17] Although there still remain some disagreements between experimental and theoretical spectra, all available evidence shows that the strong absorption at 250 nm corresponds to the $2^1A' \leftarrow 1^1A'$ transition. The weak absorption, which may be attributed to the $1^1A'' \leftarrow 1^1A'$ transition, lies above 300 nm.

Along with atmospheric interest, HOCl has many advantages to study the fundamentals of molecular photodissociation. Simple triatomic structure allows high-level ab initio calculations of the electronic states. Spectroscopic constants of the two photofragments, OH and Cl, are well-known. Since HOCl has a C_s symmetry, the electronic states are either symmetric (A′) or antisymmetric (A″) with respect to the molecular plane. The transition dipole moment of HOCl lies in the molecular plane in the case of the $2^1A' \leftarrow 1^1A'$ transition while it is perpendicular to the plane in the case of the $1^1A'' \leftarrow 1^1A'$ transition. At 248 and 266 nm, Frey and co-workers investigated the rotational alignment of the nascent OH fragment.[18−20] They obtained a negative value of the quadrupole alignment parameter $A_0^{(2)}$, which implies that the transition moment lies in the molecular plane, supporting the assignment of the absorption band at 250 nm to the $2^1A' \leftarrow 1^1A'$ transition. On the contrary, it remains obscure whether the weak absorption above 300 nm corresponds to the $1^1A'' \leftarrow 1^1A'$ transition.

The purpose of this work is to characterize the excited states of HOCl in its ultraviolet absorption spectrum. The OH fragments are observed by laser-induced fluorescence following the 266 and 355 nm photolysis. Most of the available energy is released into the kinetic energy of the photofragments, and the spectral lines show large Doppler widths. On the basis of the spectral profiles, we discuss the vector correlations ($\boldsymbol{\mu}$, **v**) and ($\boldsymbol{\mu}$, **J**) associated with the dissociation process; $\boldsymbol{\mu}$ is the transition dipole moment of HOCl, and **v** and **J** are the recoil velocity and angular momentum of the OH fragment, respectively. We show evidence that two different excited states lie in the ultraviolet region.

2. Experimental Section

Figure 1 shows a schematic diagram of the experimental setup. Two laser systems were used. (1) The fixed wavelength of Nd^{3+}:YAG laser (Continuum Surelite II) on harmonics for photodissociating HOCl at 355 or 266 nm: The photolysis laser light was linearly polarized with its electronic vector lying horizontally. The output was 70 mJ/pulse at 355 nm and 30 mJ/pulse at 266 nm. We used a stack of 12 quartz plates placed at Brewster's angle to clean up the polarization. The polarization degree (>99%) was checked in front of the entrance window of the cell. (2) A tunable laser for probing the OH fragments by laser-induced fluorescence: The 355 nm output

S1089-5639(98)00647-1 CCC: $15.00
Published on Web 05/07/1998

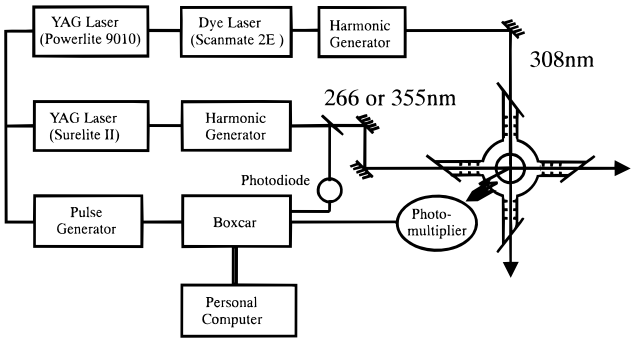

Figure 1. Experimental setup for detecting the OH fragment by laser-induced fluorescence in the photolysis of HOCl.

of a Nd^{3+}:YAG laser (Continuum Powerlite, 9010) was used to pump a dye laser (Lambda Physik, SCANmate 2). The visible radiation was doubled in a BBO crystal to excite OH in the $A^2\Sigma^+-X^2\Pi$ (0−0) band at around 308 nm with 0.04 cm^{-1} resolution. The UV output was kept low (<10 μJ/pulse) to avoid the saturation effects and power broadening. The polarization angle of the probe laser was adjusted by rotating a $\lambda/2$ plate to make the geometry of electric vectors of photolysis (ϵ^p) and analyzing-probe (ϵ^a) pulses either parallel or perpendicular; $\epsilon^p \parallel \epsilon^a$ or $\epsilon^p \perp \epsilon^a$. On the other hand, the propagating directions of the photolysis pulse (k^p) and the analyzing-probe pulse (k^a) took the following two geometries: the photolysis and probe beams counterpropagated along an axis ($k^p \parallel k^a$) or crossed at right angles ($k^p \perp k^a$). The delay between two laser pulses was controlled by a digital delay generator (Stanford Research Systems, DG-535) to make collision effects negligible (Δt = 30 ns). The fluorescence of OH was collected with a quartz lens at right angles to photolysis and probe lasers and detected by a photomultiplier (Hamamatsu Photonics, 1P28) through a 308 nm interference filter ($\Delta\lambda$ = 10 nm). The photomultiplier signals were averaged by a boxcar integrator (Stanford Research Systems SR250) and processed by a personal computer.

HOCl samples were prepared by flowing pure Cl_2 gas saturated with H_2O vapor through a HgO column. In this procedure, Cl_2O generated from the reaction of HgO + Cl_2 gave HOCl in the equilibrium reaction $Cl_2O + H_2O \rightleftarrows 2HOCl$. This mixture was slowly introduced into a photolysis cell at a pressure of 0.1−0.2 Torr. The flow system was operated under stable conditions for several hours.

3. Results and Discussion

First, we carried out an experiment with low (~0.2 cm^{-1}) resolution and found the following facts for the photodissociation of HOCl to OH + Cl. (i) The OH fragment is vibrationally cold in both 266 and 355 nm photolysis. We could not observe a trace of OH in the vibrationally excited state. (ii) The spin−orbit population ratio of OH shows a preference for $^2\Pi_{3/2}$, with a ratio of $^2\Pi_{3/2}/^2\Pi_{1/2}$ = 2.0 at 266 nm and 1.5 at 355 nm. (iii) The OH rotational population in the $^2\Pi_{3/2}$ and $^2\Pi_{1/2}$ states can be approximated by a Boltzmann distribution. The Boltzmann temperature is 800 K for $^2\Pi_{3/2}$ and 770 K for $^2\Pi_{1/2}$ in the 266 nm photolysis and 530 K for $^2\Pi_{3/2}$ and 510 K for $^2\Pi_{1/2}$ in the 355 nm photolysis.

Second, we have chosen the $R_2(1)$ line of OH to elucidate the vector correlation ($\boldsymbol{\mu}$, **v**) from the anisotropy of OH photofragments for two reasons: (i) It is well separated from other rotational lines. (ii) It is insensitive to other vector correlations ($\boldsymbol{\mu}$, **J**) and (**v**, **J**).[21] Figure 2 shows the line shape observed in the 266 nm photolysis under two different photolysis/probe geometries: (a) ($k^p \parallel k^a$ and $\epsilon^p \perp k^a$) and (b) ($k^p \perp k^a$ and $\epsilon^p \parallel k^a$). Both spectra are characterized by large line widths due to Doppler effect resulting from the recoil of the fragment. The anisotropy of the recoil velocity produces a marked difference in the two Doppler profiles. Figure 2a shows a single-peaked profile, and Figure 2b shows a double-peaked profile, indicating that **v** predominantly aligns to ϵ^p.

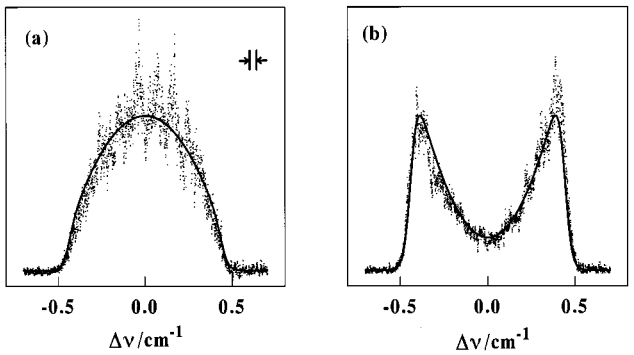

Figure 2. Doppler profiles of $R_2(1)$ line of OH in the 266 nm photolysis. The experimental geometries were (a) $k^p \parallel k^a$ and $\epsilon^p \perp k^a$ and (b) $k^p \perp k^a$ and $\epsilon^p \parallel k^a$. The dots show the experimental spectra, and the solid lines show the simulated ones with $\Delta\nu_D$ = 0.44 cm^{-1} and β = 1.3. The bandwidth of the probe laser (0.04 cm^{-1}) is shown by arrows.

A quantitative understanding of our observation is attained by examining the spatial distribution of fragments in the perpendicular and parallel transitions. According to the theory of Zare and Herschbach,[22] the Doppler profile $F(\Delta\nu)$ of photofragments with a velocity V is given by

$$F(\Delta\nu) = (1/\Delta\nu_D)[1 + \beta P_2(\cos\theta)P_2(\Delta\nu/\Delta\nu_D)] \quad (5)$$

where $\Delta\nu$ is the displacement from the line center ν_0, $\Delta\nu_D = \nu_0 V/c$ is the Doppler shift, β is the anisotropy parameter, θ is the angle between the photolysis polarization axis ϵ^p and the probe laser axis k^a, and $P_2(x) = (3x^2 - 1)/2$. We calculated the Doppler profiles by convoluting $F(\Delta\nu)$ with the parent HOCl Doppler motion at 298 K and the probe laser profile (0.04 cm^{-1}). The line profile observed under the condition $\epsilon^p \parallel k^a$ was quite sensitive to the anisotropy parameter, and the 16 measurements gave $\beta = 1.31 \pm 0.12$ at the total pressure of 0.10−0.16 Torr. This value reproduced the line profile observed at $\epsilon^p \perp k^a$ as shown in Figure 2b. All of the observed spectra showed the Doppler width of $\Delta\nu_D$ = 0.44 cm^{-1}, which indicated the recoil velocity of the OH fragments to be 4100 m/s.

The positive β value suggests parallel alignment of the transition moment and the recoil axis. Since the ground state is of A′ symmetry, this finding confirms the symmetry of the excited state to be A′. This is consistent with a theoretical predictions that the $2^1A'-1^1A'$ transition dominates the strong absorption around 250 nm. However, the measured β value is smaller than the upper limit of +2 expected for the parallel transition.

This reduction in the β value cannot be attributed to nonzero lifetime in the $2^1A'$ excited state. According to theoretical studies, all singlet excited states of HOCl in the ultraviolet region are strongly repulsive in the O−Cl coordinate, and the dissociation is direct. The OH fragments are expected to recoil along the axis of the O−Cl bond with the small rotational excitation, which was experimentally and theoretically confirmed.[15−20] Furthermore, since the OH recoil velocity (4100 m/s) is by 1 order of magnitude larger than the tangential velocity by the rotation of parent molecule (300 m/s), the OH

fragments do not attain a substantial tangential velocity to deflect the recoil axis.

A plausible explanation is that the transition moment contains a small component perpendicular to the O−Cl bond. In a simple diatomic approximation, the value of β is related to the angle χ between $\boldsymbol{\mu}$ and $\mathbf{v}$[23,24]

$$\beta = 2P_2(\cos\chi) \tag{6}$$

and the relation of $\chi = 28 \pm 3°$ is obtained from the value of $\beta = 1.31 \pm 0.12$. In ab initio calculations, Jaffe and Langhoff predicted that the $2^1A'-1^1A'$ system was dominated by the transition moment parallel to the O−Cl axis.[14] However, there is a contribution of the perpendicular transition component lying in the molecular plane. The transition moment is estimated to incline at an angle of 7−25° from the O−Cl axis depending on the basis set and molecular geometry used in the calculations. On the other hand, a recent ab initio calculation by Nanbu and Iwata showed that the absorption band that peaked at 245 nm resulted from two transitions, $2^1A'-1^1A'$ and $2^1A''-1^1A'$.[15] As for the transition moment of the $2^1A'-1^1A'$ system, the component perpendicular to the O−Cl bond predominated over the parallel component. Since the $2^1A''-1^1A'$ transition only became important at higher energies, this calculation placed the transition moment in the molecular plane, making the angle of ∼85° with respect to the O−Cl axis at 266 nm. Our result agrees with the prediction by Jaffe and Langhoff in terms of the existence of a small perpendicular transition moment in the $2^1A'-1^1A'$ system, but not with that by Nanbu and Iwata.

Frey and co-workers studied the photodissociation dynamics of HOCl from the internal energy distribution of OH and Cl.[18−20,25] They observed the spectra of the OH fragment by laser-induced fluorescence in the photolysis at 248 and 266 nm. The excitation spectra were characterized by the negative rotational alignment parameter $A_0^{(2)}$, and the OH fragments showed the preferential production of the Π(A′) lamda doublet state with an increase of rotational quantum number. These results showed the transition moment lying in the molecular plane and agreed with the $2^1A'-1^1A'$ transition at 248 and 266 nm.[18−20] However, they reported that the Cl atoms with their initial velocities aligned in the plane perpendicular to the photolysis laser polarization for the 235 nm photolysis, implying that the transition moment was perpendicular to the O−Cl axis.[25] This conclusion is obviously in conflict with our observation. To solve the problem, we have recently studied the photodissociation of HOCl by using the photofragment imaging technique.[26] HOCl was photodissociated at 235 nm using the second harmonics of a dye laser, and the same pulse was used to ionize the Cl fragments in the (2 + 1) multiphoton absorption. The spacial distribution of Cl^+ ions showed that the Cl fragments recoiled along the electronic vector of the photolysis laser. The anisotropy parameter $\beta = 1.7 \pm 0.2$ is close to the upper limit of 2 for the parallel transition. Since this result is consistent with the observation presented in this paper, the transition at 235 nm is attributed to the same electronic transition at 266 nm. The theoretical calculations ensured this point of view.[14,15] The β value is slightly different from the present study, since HOCl is photolyzed at shorter wavelengths. In the $2^1A' \leftarrow 1^1A'$ system, the direction of the transition moment (and accordingly the value of β) is predicted to show the wavelength dependence by the theoretical calculation (Figure 9 in ref 15).

Figure 3 shows the Doppler profiles of the $R_2(1)$ transition observed in the 355 nm photolysis. The dependence of the profiles on the photolysis/probe geometry is contrary to that of the 266 nm photolysis. Namely, the $R_2(1)$ line showed a double-peaked profile in spectrum a under the conditions of (k^p || k^a and $\epsilon^p \perp k^a$), while a single-peaked one in spectrum b under the conditions of ($k^p \perp k^a$ and ϵ^p || k^a). This result indicates that **v** is predominantly aligned perpendicular to ϵ^p, not along ϵ^p. The Doppler profiles in spectra a and b are reproduced by $\Delta\nu_D = 0.31$ cm^{-1} and $\beta = -0.7$. The Doppler width $\Delta\nu_D = 0.31$ cm^{-1} indicates that the OH fragments recoil with a velocity of 2900 m/s. The 44 measurements gave the value of $\beta = -0.70 \pm 0.12$ under the total pressure of 0.09−0.21 Torr.

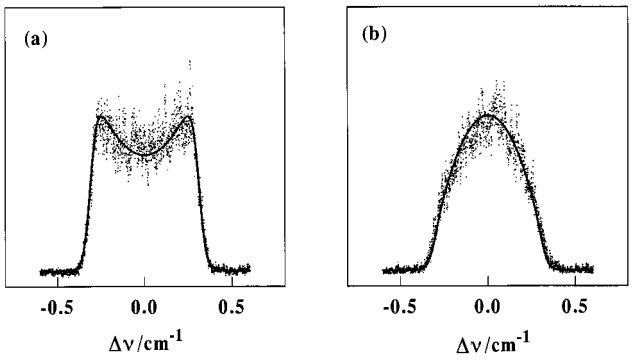

Figure 3. Doppler profiles of $R_2(1)$ line of OH in the 355 nm photolysis. The experimental geometries (a) k^p || k^a and $\epsilon^p \perp k^a$ and (b) $k^p \perp k^a$ and ϵ^p || k^a. The dots show the experimental spectra, and the solid lines show simulated ones with $\Delta\nu_D = 0.31$ cm^{-1} and $\beta = -0.7$.

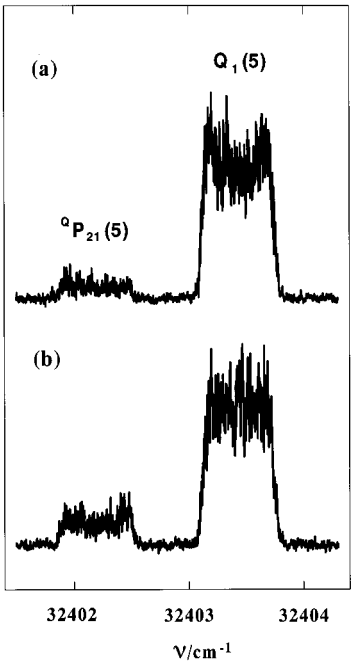

Figure 4. The main transition $Q_1(5)$ and accompanying satellite line $^QP_{21}(5)$ in the 355 nm photolysis of HOCl observed at two photolysis/probe geometries: (a) (k^p || k^a and ϵ^p || ϵ^a) and (b) (k^p || k^a and $\epsilon^p \perp \epsilon^a$).

The β value is obviously negative, suggesting that the transition moment of HOCl at 355 nm is perpendicular to the O−Cl bond. At first sight, this conclusion is consistent with the recent predictions that the $1^1A''-1^1A'$ lies at wavelengths longer than 300 nm. However, we still cannot exclude the possibility that the transition moment is perpendicular to the O−Cl bond, but that it lies in the molecular plane.

To clarify this point, we studied the vector correlation, ($\boldsymbol{\mu}$, **J**), between the transition moment and the rotation vector of the fragment. Figure 4 shows a typical example of the spectra, showing the main $Q_1(5)$ transition and the accompanying satellite $^QP_{21}(5)$ line recorded with two photolysis/probe

geometries: (a) (k^p || k^a and ϵ^p || ϵ^a) and (b) (k^p || k^a and $\epsilon^p \perp \epsilon^a$). The Q-branch transition obviously shows the reduction of the central dip in spectrum b owing to the (**v**, **J**) correlation. Apart from the change of the Doppler profile, it is more important here to realize that the satellite P line increases in intensity relative to the main Q-branch transition, when we compared spectrum b with spectrum a. This phenomenon occurs due to the ($\boldsymbol{\mu}$, **J**) correlation. The alignment of $\mathbf{J}_{OH}$ to $\boldsymbol{\mu}$ is quantitatively derived from the polarization dependence of the intensity ratios between the P (or R)- and Q-branch transitions originating from the same lower state. By the treatments in the literature,[27,28] we obtained the rotational alignment parameter $A_0^{(2)} \sim 0.3$ at $N = 5$ from the results shown in Figure 4. The $A_0^{(2)}$ value is *J*-dependent. At the high *J* limit $A_0^{(2)}$ may take the values $+4/5$ ($\boldsymbol{\mu}$ || **J**) and $-2/5$ ($\boldsymbol{\mu} \perp$ **J**). Since the dissociation of HOCl occurs by repulsive impulse along the O−Cl bond, $\mathbf{J}_{OH}$ is perpendicular to the molecular plane. The positive $A_0^{(2)}$ value shows a preferential parallel alignment of $\boldsymbol{\mu}$ and $\mathbf{J}_{OH}$, indicating the transition moment being perpendicular to the molecular plane at 355 nm. This result indicates that the $1^1A'' \leftarrow 1^1A'$ transition dominates the absorption spectrum at 355 nm.

The anisotropy parameter of $\beta = -0.70 \pm 0.12$ at 355 nm is slightly smaller than the lower limit of -1 for the perpendicular transition. This fact might indicate that the absorption is composed of the main $1^1A'' \leftarrow 1^1A'$ transition and an additional transition whose transition moment is parallel to the O−Cl axis. At present, we can suggest two possibilities for the additional transition. One is a contribution of the $2^1A' \leftarrow 1^1A'$ system. The $1^1A'' \leftarrow 1^1A'$ system is weak, and the tail of the strong $2^1A' \leftarrow 1^1A'$ band may still have a notable contribution at 355 nm. Assuming $\beta = 1.3$ at 355 nm for the $2^1A' \leftarrow 1^1A'$ transition obtained in this study, we can estimate that the 87% of the absorption at 355 nm goes through the $1^1A''$ state and 13% through the $2^1A'$ state. Another possibility is a contribution of the $1^3A'' \leftarrow 1^1A'$ system. In the case of HOBr, Sinha et al. have recently found the weak transition between 440 and 660 nm, whose transition moment is dominantly parallel to the HO−Br bond.[29,30] They assigned this band to the excitation to the lowest triplet state of A″ symmetry which borrows intensity from nearby singlet state(s) of A′ character through spin−orbit interaction. In the case of HOCl, the spin−orbit coupling between singlet and triplet states should be small compared with that found in HOBr, but we cannot exclude this possibility at the present stage.

The Doppler widths of OH fragment are related to the dissociation energy of the O−Cl bond (E_{diss}). In the 266 nm photolysis, the energy conservation requires that

$$E_{h\nu} + E_{HOCl,int} = E_{diss} + E_{trans} + E_{OH,int} + E_{Cl,int} \quad (7)$$

where the energy of the photolysis laser light ($E_{h\nu}$) is 37 577 cm^{-1}. The averaged thermal internal energy of the parent HOCl ($E_{HOCl,\ int}$) is 340 cm^{-1}. E_{trans} is the total translational energy of the OH and Cl fragments. The internal energy of $^2\Pi_{1/2}(1)$ state ($E_{OH,\ int}$) is calculated to be 126 cm^{-1} from the spectroscopic constants.[31] In the photolysis of HOCl at around 236 nm, Bell et al. reported a ratio of 0.30 ± 0.07 for Cl $^2P_{1/2}$:$^2P_{3/2}$ with a 881 cm^{-1} energy separation.[25] Assuming that this branching ratio still held for two isotope species, ^{35}Cl and ^{37}Cl with a 3:1 ratio, we attempted to convolute the recorded line shapes using four different velocity components originating from the two isotopes in the ground and excited states. The calculations were carried out for E_{diss} with a 1000 cm^{-1} interval, and we found that the spectra observed in the 266 nm photolysis can be reproduced with $E_{diss} = 19\,000 \pm 1000$ cm^{-1}, which is consistent with the recently reported values of $19\,290.3 \pm 0.6$ and $19\,288.8 \pm 0.6$ cm^{-1}.[32,33]

4. Conclusion

We have investigated the electronically excited states of HOCl by observing the anisotropy of OH photofragments. Two different electronic transitions were identified in the ultraviolet region: one is the $2^1A' \leftarrow 1^1A'$ transition observed at 266 nm, and the other is the $1^1A'' \leftarrow 1^1A'$ transition at 355 nm. This is the first experimental evidence for the $1^1A'' \leftarrow 1^1A'$ transition existing in HOCl above 300 nm.

Acknowledgment. The work is partly supported by a Hiroshima City University Grant for Special Academic Research (General Studies). T.I. is grateful to a Grant-in-Aid for Scientific Research from the Ministry of Education, Science, Sports and Culture. The authors acknowledge Prof. M. Kawasaki for valuable discussions and comments.

References and Notes

(1) Rowland, F. S.; Molina, M. J. *Rev. Geophys. Space Phys.* **1975**, *13*, 1.
(2) Warneck, P. *Z. Naturforsch. A* **1977**, *32*, 1254.
(3) Abbatt, J. P. D.; Molina, M. J. *J. Phys. Chem.* **1992**, *96*, 7674.
(4) Atkinson, R.; Baulch, D. L.; Cox, R. A.; Hampson, R. F., Jr.; Kerr, J. A.; Rossi, M. J.; Troe, J. *J. Phys. Chem. Ref. Data* **1997**, *26*, 521.
(5) *CRC Handbook of Chemistry and Physics*, 76th ed.; Lide, D. R., Frederikse, H. P. R., Eds.; CRC Press: Boca Raton, FL, 1995.
(6) Molina, M. J.; Ishiwata, T.; Molina, L. T. *J. Phys. Chem*. **1980**, *84*, 3100.
(7) Butler, P. J. D.; Phillips, L. F. *J. Phys. Chem.* **1983**, *87*, 183.
(8) Vogt, R.; Schneider, R. N. *J. Photochem. Photobiol. A* **1992**, *66*, 133.
(9) Molina, L. T.; Molina, M. J. *J. Chem. Phys.* **1978**, *82*, 2410.
(10) Knauth, H.-D.; Alberti, H.; Clausen, H. *J. Phys. Chem.* **1979**, *83*, 1604.
(11) Mishalanie, E. A.; Rutkowski, C. J.; Hutte, G.; Birks, J. W. *J. Phys. Chem.* **1986**, *90*, 5578.
(12) Jungkamp, T. P. W.; Kirchner, U.; Schmidt, M.; Schindler, R. N. *J. Photochem. Photobiol. A* **1995**, *91*, 1.
(13) Hirsch, G.; Bruna, P. J.; Peyerimhoff, S. D.; Buenker, R. J. *Chem. Phys. Lett.* **1977**, *52*, 442.
(14) Jaffe, R. J.; Langhoff, R. *J. Chem. Phys.* **1978**, *68*, 1638.
(15) Nanbu, S.; Iwata, S. *J. Phys. Chem.* **1992**, *96*, 2103.
(16) Guo, H. *J. Phys. Chem.* **1993**, *97*, 2602.
(17) Offer, A. R.; Balint-Kurti, G. G. *J. Chem. Phys.* **1996**, *104*, 563 and references therein.
(18) Bell, A. J.; Pardon, P. R.; Hickman, C. G.; Frey, J. G. *J. Chem. Soc., Faraday Trans.* **1990**, *86*, 3831.
(19) Hickman, C. G.; Brickell, A.; Frey, J. G. *Chem. Phys. Lett.* **1991**, *185*, 101.
(20) Hickman, C. G.; Shaw, N.; Crawford, M. J.; Bell, A. J.; Frey, J. G. *J. Chem. Soc., Faraday Trans.* **1993**, *89*, 1623.
(21) Docker, M. P.; Hodgson, A.; Simons, J. P. *Chem. Phys. Lett.* **1986**, *128*, 264.
(22) Zare, R. N.; Herschbach, D. R. *Proc. IEEE* **1963**, *51*, 173.
(23) Dubs, M.; Brühlmann, U.; Robert Huber, J. *J. Chem. Phys.* **1986**, *84*, 3106.
(24) Dixon, R. N. *J. Chem. Phys.* **1986**, *85*, 1866.
(25) Bell, A. J.; Boggis, S. A.; Dyke, J. M.; Frey, J. G.; Richter, R.; Shaw, N.; Tabrizchi, M. *J. Chem. Soc., Faraday Trans.* **1994**, *90*, 17.
(26) Tanaka, Y.; Kawasaki, M.; Matsumi, Y.; Fujiwara, H.; Ishiwata, T.; Rogers, L. J.; Dixon, R. N.; Ashfold, M. N. R., to be published.
(27) Greene, C. G.; Zare, R. N. *J. Chem. Phys.* **1983**, *78*, 6741.
(28) Vasudev, R.; Zare, R. N.; Dixon, R. N. *J. Chem. Phys.* **1984**, *80*, 4863.
(29) Barnes R. J.; Lock, M.; Coleman J.; Sinha, A. *J. Phys. Chem.* **1996**, *100*, 453.
(30) Lock, M.; Barnes R. J.; Sinha, A. *J. Phys. Chem.* **1996**, *100*, 7972.
(31) Dieke, G. H.; Crosswhite, H. M. *J. Quant. Spectrosc. Radiat. Transfer* **1962**, *2*, 97.
(32) Wedlock, M. R.; Jost, R.; Rizzo, T. R. *J. Chem. Phys.* **1997**, *107*, 10344.
(33) Barnes, R. J.; Dutton G.; Sinha, A. *J. Phys. Chem. A* **1997**, *101*, 8374.